bcl-2 acts early to restrict Semliki Forest virus replication and delays virus-induced programmed cell death

JOURNAL OF VIROLOGY, Feb. 1997, p. 1583–1590 Vol. 71, No. 2
0022-538X/97/$04.00+0

bcl-2 Acts Early To Restrict Semliki Forest Virus Replication and Delays Virus-Induced Programmed Cell Death

MARTINA F. SCALLAN, TIMOTHY E. ALLSOPP, AND JOHN K. FAZAKERLEY*

Department of Veterinary Pathology, University of Edinburgh, Edinburgh EH9 1QP, United Kingdom

Received 10 June 1996/Accepted 15 October 1996

As characterized by morphological assessment and terminal deoxynucleotidyltransferase-mediated dUTP nick end labeling, Semliki Forest virus (SFV) infection of rat prostatic adenocarcinoma cells triggers an apoptotic cell response. Cell death proceeded more rapidly following infection with the neurovirulent L10 strain of SFV than with the avirulent A7 strain. Overexpression of the antiapoptotic proto-oncogene *bcl-2* allowed survival of cultures infected with either strain of virus. *bcl-2* overexpression drastically reduced the numbers of productively infected cells within the cultures. In situ hybridization for viral message-sense RNA coupled with immunostaining for viral protein indicated that *bcl-2* functions at an early stage of the virus life cycle, at entry, pretranscriptional events or at transcription, to inhibit virus replication. Double-immunofluorescent labeling for *bcl-2* and viral glycoproteins revealed double-positive cells, demonstrating that with time, this early block in replication can be overcome. These productively infected *bcl-2*-expressing cells do, with time, undergo apoptosis. As a result of changing the balance between cell death and cell division by restricting productive virus replication and delaying virus-induced cell death, *bcl-2* expression led to the establishment of chronically infected cell lines which could be passaged.

The avirulent A7 and virulent L10 strains of Semliki Forest virus (SFV) display the same cell tropism in the central nervous system (CNS) of 3- to 4-week-old mice, with neurons and oligodendrocytes as the primary target cells (reference 26 and our unpublished observations). However, the rates of spread of these two strains within the CNS differ markedly. Following intraperitoneal infection, the A7 strain fails to spread from its perivascular sites of entry in the CNS and remains confined to small foci scattered throughout the brain and spinal cord. Immunocompetent mice clear these foci within 2 weeks of infection. In contrast, the L10 strain, which also initiates CNS infection as small perivascular foci, spreads rapidly throughout the brain and spinal cord, resulting in acute encephalitis and death of the mouse within 5 days (7).

In neonatal mice, SFV A7 spreads rapidly through the CNS (7, 21). This change in spread correlates with the age-related virulence characteristic of this strain of SFV (3, 23). SFV A7 infection of mice younger than 14 days results in 100% mortality (21). This age-related susceptibility to SFV A7 cannot be accounted for by maturing immune responses, since intraperitoneal inoculation of 3- to 4-week-old SCID mice results in a persistent CNS infection which remains focal, with no dissemination of the virus (1). Failure to clear virus from peripheral tissues gives rise to a persistent viremia which continuously seeds foci of infection in the CNS. Despite the accumulation of significant levels of viral RNA and protein inside cells within these foci, most mature CNS cells remain morphologically intact. This is in marked contrast to the cytopathology observed following SFV A7 infection of neonatal CNS cells in vivo. Similar observations of age-related virulence have been made with strains of Sindbis virus (10, 12).

Electron microscopic (EM) analyses have demonstrated complete replication, including budding virions in the CNS of neonatal mice infected with SFV A7. However, detailed EM examination of A7-infected adult mouse brain has consistently highlighted the absence of advanced stages of virus replication in mature CNS cells (7, 23, 24). SFV A7-positive cells within the developed CNS contain amorphous aggregates of viral material termed viral core aggregates, but no assembled virions have ever been observed. Within mature neurons, SFV A7 replication is restricted (7). In mature SCID or athymic *nu*/*nu* mice, CNS neurons containing viral RNA can be detected for the lifetime of the animal (1, 9).

Neurons are essential, irreplaceable components of the mature CNS. Since neuronal destruction constitutes irreversible pathology, it is imperative that these highly specialized cells are preserved. It has become clear that some virus infections can induce programmed cell death. This has been illustrated with members of the *Herpesviridae* (13), *Parvoviridae* (20), *Retroviridae* (16, 19), *Paramyxoviridae* (6), *Myxoviridae* (11), and *Picornaviridae* (27) and with the prototype alphavirus, Sindbis virus (18). A number of mammalian genes encoding antagonists of programmed cell death have been identified. Among those described, *bcl-2* and *bcl-x* are known to be expressed in the CNS. There is now evidence supporting a role for these genes in promoting the survival of mature CNS neurons (14). It is conceivable that by rendering mature CNS cells refractory to virus-induced programmed cell death, genes of the *bcl-2* family may inadvertently allow neurons to act as reservoirs of viral material.

Evidence to date suggests that developmentally regulated host cell factors influence the outcome of SFV A7 infection in vivo, in terms of cytopathology and virus propagation (7, 21). Levine and coworkers reported that Sindbis virus induces apoptosis upon infection of rat prostatic adenocarcinoma cells (AT3 cells) and that this virus-induced programmed cell death can be prevented by overexpression of the cellular oncogene *bcl-2* (18). They demonstrated that *bcl-2* expression led to the establishment of a persistent infection. We have used the same transfected AT3 cell lines to determine whether SFV infection induces programmed cell death and to investigate in detail the effect of overexpression of *bcl-2* on the outcome of this infection.

* Corresponding author. Mailing address: Department of Veterinary Pathology, University of Edinburgh, Summerhall, Edinburgh EH9 1QP, United Kingdom. Phone: 0131 650 6160. Fax: 0131 650 6511. E-mail: John.Fazakerley@ed.ac.uk.

MATERIALS AND METHODS

Cells. AT3 cell lines transfected with the expression vector pZipNeo (AT3Neo [4]) or the recombinant plasmid pZipBcl-2 (AT3Bcl-2 [18]) were obtained from Marie Hardwick (Johns Hopkins University School of Medicine, Baltimore, Md.). Cell cultures were maintained at 37°C in supplemented RPMI. Cell viability was assessed by trypan blue exclusion at serial time points after SFV infection.

Viruses and plaque assays. Highly purified virus was used in these experiments to avoid potential effects due to factors such as cytokines, for example, interferons, which could be present in crude virus preparations such as infected cell supernatants. Infected culture supernatants were harvested 48 h postinfection from BHK cell monolayers (infected at 0.01 PFU/ml) and clarified by centrifugation at 7,000 rpm (4°C) in a Sorval GSA rotor for 20 min. Virus was precipitated overnight (with 23 g of NaCl and 70 g of polyethylene glycol 8000 per liter) from clarified culture supernatant maintained at 4°C. Precipitated virus was pelleted by centrifugation (as before) and resuspended in low-salt buffer (LSB; 0.15 M NaCl, 10 mM Tris [pH 7.4]). The virus suspension was loaded onto preformed 20 to 70% sucrose gradients prepared in clear SW41 tubes and banded by centrifugation for 2 h at 35,000 rpm in a Beckman ultracentrifuge at 4°C. The virus band (formed in the middle of the gradient) was harvested, diluted with LSB, and pelleted for 1 h at 35,000 rpm (4°C) in an SW41 rotor. The virus pellet was resuspended in a small volume of LSB. All plaque assays were performed on 80% confluent BHK cell monolayers as described previously (7).

EM analyses. Cells were fixed in tissue culture flasks with 3% glutaraldehyde in 0.1 M sodium cacodylate buffer (pH 7.3), scraped into the buffered fixative, and pelleted by centrifugation at $1,000 \times g$ for 5 min. Postfixation, the cell pellets were immersed in 1% osmium tetroxide in 0.1 M sodium cacodylate buffer, dehydrated through graded acetones (50 to 100%), and embedded in araldite resin. Semithin (1-μm) sections were cut, stained with toluidine blue and borax, and examined by light microscopy. Ultrathin sections for EM analysis were stained with uranyl acetate and lead citrate and examined in a Philips EM400 transmission microscope.

Immunostains. Viral glycoproteins were detected by using a mixture of two monospecific rabbit antipeptide antisera specific for SFV E1 and E2, followed by a biotinylated goat anti-rabbit immunoglobulin G as secondary antibody (Vector Laboratories), an avidin-biotin-peroxidase amplification step (Vector), and diaminobenzidine (Sigma) as the substrate. Cultures to be immunostained were grown on poly-L-lysine-coated dual-chamber slides (Nunc) and fixed with 2% paraformaldehyde-lysine-periodate fixative (PLP) or 4% phosphate-buffered formal saline (PBS). Immunofluorescent staining for *bcl-2* protein was performed with an anti-human monoclonal antibody (MCA1279; Serotec) and a rhodamine isothiocyanate-conjugated goat anti-mouse secondary antibody. Fluorescent staining for viral glycoproteins was performed with the antipeptide antiserum followed by a fluorescein isothiocyanate-conjugated anti-rabbit antiserum (Dako).

TUNEL. PLP-fixed chamber slide cultures of AT3 cells were rinsed with PBS and permeabilized with 0.3% Triton X-100 in PBS for 10 min. One specimen was designated a positive control, equilibrated with DNase I buffer (30 mM Tris [pH 7.2], 140 mM sodium cacodylate, 4 mM $MgCl_2$, 0.1 mM dithiothreitol) for 20 min, and then incubated in this buffer with DNase I (5 μg/ml) at 37°C for 30 min. After permeabilization, the remaining specimens were rinsed with PBS and equilibrated with terminal deoxynucleotidyltransferase (TdT)-mediated dUTP nick end-labeling (TUNEL) buffer (30 mM Tris [pH 7.2], 140 mM sodium cacodylate, 1 mM cobalt chloride) for 20 min. All specimens were incubated with TdT (0.3 U/μl), 20 μM digoxigenin (DIG)-11-dUTP, 30 mM Tris (pH 7.2), 140 mM sodium cacodylate, and 1 mM cobalt chloride for 2 h at 37°C in a humidified container. As a negative control, TdT enzyme was omitted from one reaction. The reaction was terminated with 2× SSC (1× SSC is 0.15 M NaCl plus 0.15 M sodium citrate) for 5 min at room temperature. Incorporated DIG-dUTP was detected by enzyme-linked immunoassay, using an anti-DIG-alkaline phosphatase conjugate to catalyze a color reaction between 5-bromo-4-chloro-3-indolyl phosphate (X-phosphate) and nitroblue tetrazolium salt, which deposits a blue precipitate. Specimens were equilibrated with PBS, blocked with 3% normal goat serum for 30 min, washed twice for 5 min each time in PBS–0.05% Tween 20, and incubated with anti-DIG-alkaline phosphatase conjugate (Boehringer) diluted 1:100 in PBS with 1% normal goat serum. The specimens were then washed with PBS (three times for 5 min each) and incubated with nitroblue tetrazolium salt and X-phosphate solutions as detailed in the protocol for the Boehringer detection kit (catalog no. 1175 041).

Protein radiolabeling. Eighty percent confluent BHK cell monolayers were either mock infected or infected at a multiplicity of infection (MOI) of 5 PFU/cell with SFV A7. At 10, 22, 30, and 46 h postinfection, supernatant was harvested, clarified (centrifuged at $1,000 \times g$ for 5 min), and assayed for levels of infectious virus. At each time point, monolayers were washed with PBS and pulse-labeled for 1 h with ^{35}S-Trans-label (ICN). Cell lysates were fractionated on sodium dodecyl sulfate–12% polyacrylamide gels (15). Gels were soaked in amplify (Amersham), dried under vacuum, and placed against photographic film (GRI) for autoradiography.

In situ hybridization. In situ hybridization was performed with a ^{35}S-labeled riboprobe transcribed in vitro (using a riboprobe Gemini kit; Promega) from *Hin*cII-linearized pGEM1-SFV (a kind gift from H. Garoff, Karolinska Institute, Stockholm, Sweden). Transcription with T7 polymerase yielded a radiolabeled negative-sense transcript complementary to the structural region of the SFV genome. The radiolabeled transcript underwent alkaline hydrolysis in 0.04 M $NaHCO_3$ (30 min, 60°C) prior to use. The in situ hybridization procedure was as detailed previously (7, 8) except that the Triton X-100 and proteinase K pretreatment steps were omitted. At the end of the in situ hybridization procedure, slides were dehydrated through 30 to 100% alcohol (containing 0.33 M ammonium acetate) and placed in 0.3% H_2O_2 in methanol for 30 min prior to immunostaining with the rabbit antipeptide antiserum as described above. The slides were then dipped in LM-1 emulsion and stored in the dark at 4°C. After 48 h, slides were developed with Ilford ILfosol S developer as instructed by the manufacturer.

RESULTS

SFV induces apoptosis. EM examination of SFV A7-infected AT3Neo cells revealed morphological features of apoptosis. Figure 1 displays EM images of an uninfected AT3Neo cell and an AT3Neo cell 36 h after infection with SFV A7. The nuclei of infected cells generally had condensed and marginalized chromatin, and the plasma membrane had lost the microvilli characteristic of uninfected AT3 cells and was folded dramatically, creating cytoplasmic protrusions or blebs. The cytoplasm of infected cells was shrunken and highly vacuolated (Fig. 1B). TUNEL of SFV A7-infected AT3Neo cells revealed that the nuclear DNA within these dying cells was fragmented, another feature diagnostic of apoptosis (see Fig. 5E). Immunostaining for viral glycoproteins confirmed that these cells were infected. Interestingly, the blebbed cytoplasmic protrusions held particularly high concentrations of viral glycoproteins (see Fig. 5C and E).

Toluidine blue-stained 1-μm sections of pelleted uninfected and infected AT3Neo cultures were examined by light microscopy. In Fig. 2, toluidine blue-stained sections of uninfected and infected AT3Neo cells (36 h postinfection) are compared. In general, relative to uninfected cells, cells in the infected cultures were more rounded and had pale staining cytoplasm. By 36 h, a large proportion of cells in the infected cultures displayed a darkly stained margin of beaded chromatin edging the nucleus, with the remainder of the nucleus lightly stained relative to uninfected cells (Fig. 2B). Some blebbing cells were evident in the infected cultures, and late stages of chromatin condensation into apoptotic bodies was apparent in some cells (Fig. 2B). In contrast, the nuclei and cytoplasm of uninfected cells were relatively darkly stained with toluidine blue, and chromatin was not marginalized (Fig. 2A).

***bcl-2* slows SFV-induced programmed cell death.** To determine whether the antiapoptotic gene *bcl-2* can prevent SFV-induced programmed cell death, the courses of viral infection in AT3 cells expressing this gene (AT3Bcl-2 cells) and in control AT3Neo cells were compared. Cell viabilities within SFV A7- or SFV L10-infected AT3Neo and AT3Bcl-2 cultures, and parallel uninfected cultures, were compared by trypan blue exclusion at serial time points after infection (MOI of 5 PFU/cell). With time, infected cells became less adherent and most of the cells displaying apoptotic features were floating in the culture supernatant. Viability counts were therefore performed on the total cell population by pooling monolayer cells with cells in suspension in each sample. Parallel, triplicate cultures were measured at each time point for each virus, and the study was repeated at least three times with similar results. The data presented are typical.

From 24 h, cell loss from SFV A7-infected AT3Neo cultures was observed, and by 72 h, the cultures were completely destroyed (Fig. 3A). In contrast, in the AT3Bcl-2 cultures, the number of live cells in parallel infected and mock-infected cultures increased up to 48 h (Fig. 3A). However, between 48 and 72 h, there was no increase in the number of live cells in

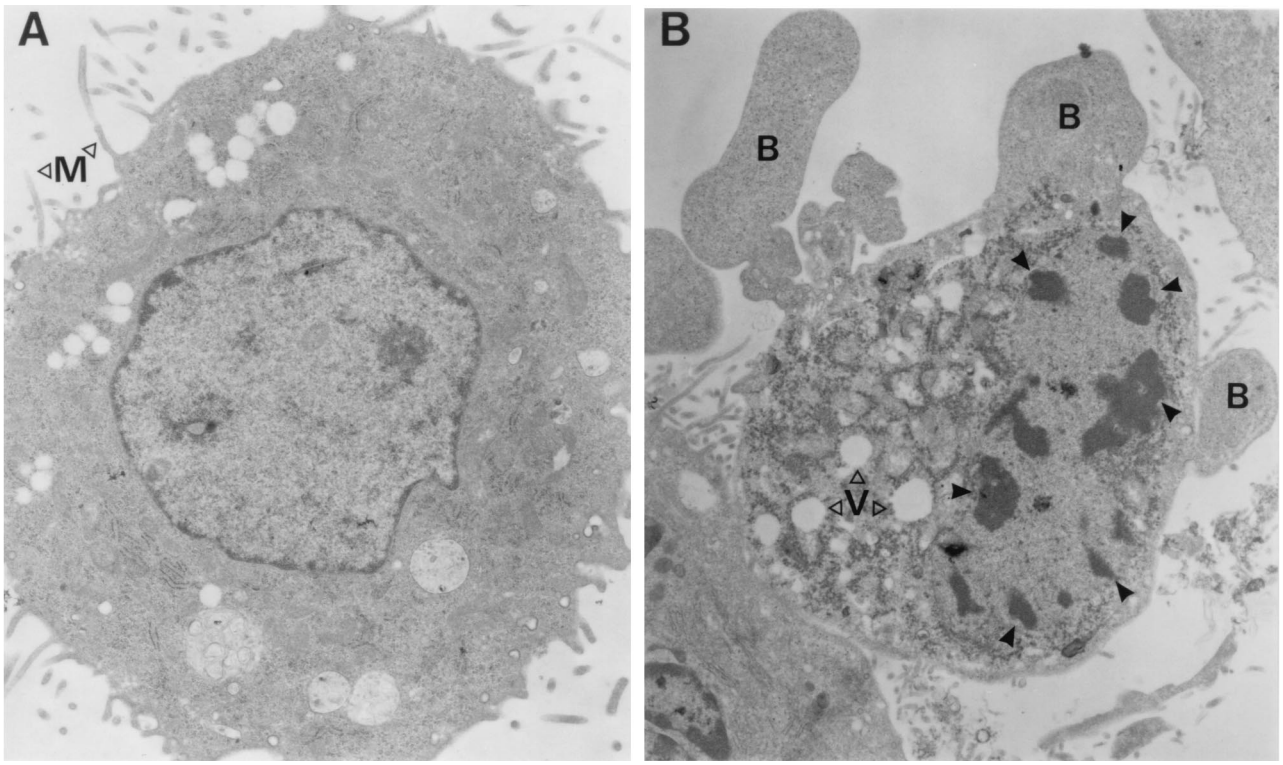

FIG. 1. EM images. (A) Uninfected AT3Neo cell (M, microvilli). (B) SFV A7-infected AT3Neo cell at 36 h postinfection, with condensed and marginalized chromatin (solid arrowheads), surface protrusions (blebs; B), and vacuolated cytoplasm (V).

SFV A7-infected AT3Bcl-2 cultures, although the parallel mock-infected cultures doubled in viable cell number over the same time period, reaching confluence at 1.4×10^6 cells per 35-mm-diameter plate by 72 h. This difference in live cell number coincided with the appearance of trypan blue-permeable cells in the infected AT3Bcl-2 cultures. Even though some cell death was evident in the infected AT3Bcl-2 cultures from this time onward, the cultures were viable and could be subcultured, giving rise to persistently infected cell lines.

AT3Neo cultures were destroyed more rapidly with SFV L10 than with SFV A7 (Fig. 3B). By 24 h, there was significant cell loss in the SFV L10-infected AT3Neo cultures relative to infected AT3Bcl-2 cultures. The AT3Neo cultures were almost totally destroyed by 36 h. However, as with SFV A7, *bcl-2* expression promoted survival of SFV L10-infected AT3 cultures (Fig. 3B). As in the SFV A7 time course, mock-infected AT3Bcl-2 cultures outgrew SFV L10-infected AT3Bcl-2 cultures, with L10 infection resulting in earlier divergence of these growth curves.

***bcl-2* expression slows virus production but allows increased virus yield.** To further compare the courses of infection in the two cell lines, the titers of infectious virus in the culture supernatants were determined. These are shown in Fig. 3C and D for SFV A7 and L10, respectively, and are from the same experiment as the cell counts. At 24 h, there were equal numbers of cells excluding trypan blue in the SFV A7-infected AT3Neo and AT3Bcl-2 cultures (Fig. 3A); however, at this time point, virus yields from the *bcl-2*-expressing cultures were 1,000-fold lower than those from the AT3Neo cultures (Fig. 3C). After 24 h, there was no further accumulation of extracellular virus in the infected AT3Neo cultures, consistent with the massive cell death occurring at this time. Extracellular virus continued to accumulate in the supernatant of infected AT3Bcl-2 cells, reaching levels similar to those in infected AT3Neo cultures by 48 h and exceeding these levels by 72 h. Initial virus yields from AT3 cells infected with SFV L10 were also reduced by expression of *bcl-2*, and as seen with SFV A7, the titer of SFV L10 virus in the supernatant of the AT3Neo cultures started to fall after 24 h as viable cells in these cultures were depleted (Fig. 3D and B). In contrast, the L10 virus titers in the surviving AT3Bcl-2 cultures showed, as with A7 titers, a steady increase with time (Fig. 3D).

Viral protein synthesis. To determine whether the difference in infectious virus titer in the supernatants of AT3Neo and AT3Bcl-2 cells was due to a difference in virus replication or virus release, virus protein synthesis was measured in the cultures. Pulse-labeling of SFV A7-infected AT3Neo cultures with ^{35}S-labeled methionine and cysteine demonstrated that by 46 h, host cell protein synthesis had shut down. From 22 h, viral proteins, particularly the viral capsid protein, could be clearly detected against the low background of host cell proteins (Fig. 4). In contrast, levels of viral protein synthesis in the SFV A7-infected AT3Bcl-2 cultures were too low to be discerned against the continuing host cell protein synthesis. Between 10 and 30 h, taking the culture as a whole, more viral proteins were synthesized in infected AT3Neo than in infected AT3Bcl-2 cultures. This result is consistent with the virus titers in the supernatant at these time points and indicates that virus replication is greatly reduced in the AT3Bcl-2 cultures.

***bcl-2* expression limits virus spread.** The virus release and pulse-labeling data demonstrate that *bcl-2* expression slows the progress of SFV infection at the level of the whole culture. To examine events at the individual cell level, duplicate, parallel SFV A7-infected AT3Neo and AT3Bcl-2 cultures were immunostained to monitor expression of the viral glycoproteins (E1 and E2). Establishment of infection in both cell lines was slow.

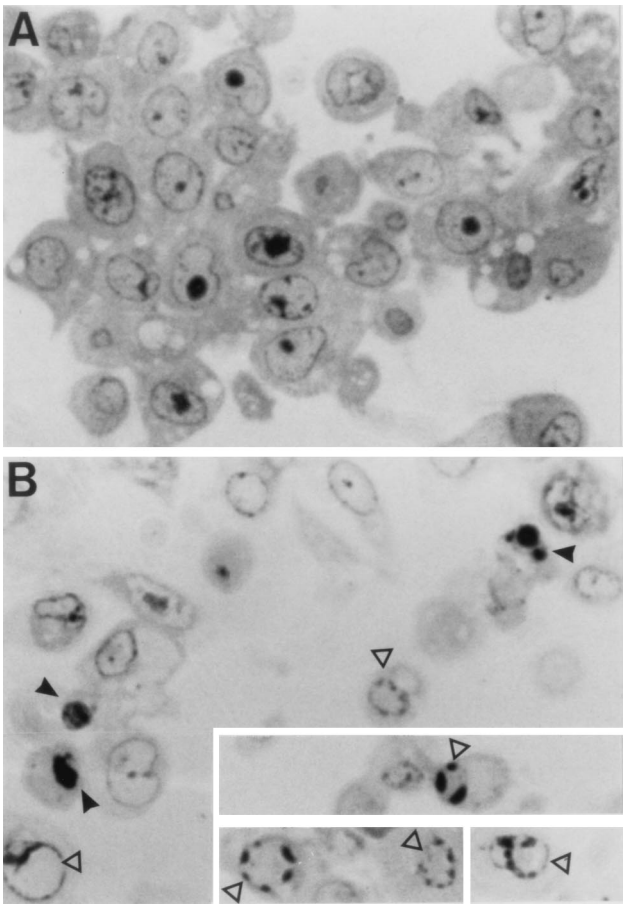

FIG. 2. Toluidine blue-stained 1-μm sections of uninfected AT3Neo cells (A) and SFV A7-infected AT3Neo cells harvested from an infected monolayer at 24 h (B). Both preparations were stained for 1.5 min. Note that the nuclei and cytoplasm of the infected cells are pale staining relative to the uninfected cells. Many infected cells have beads of perinuclear staining (arrowheads) indicative of marginalized chromatin. Cells in later stages of cell death with chromatin condensed into apoptotic bodies are also present (solid arrowheads).

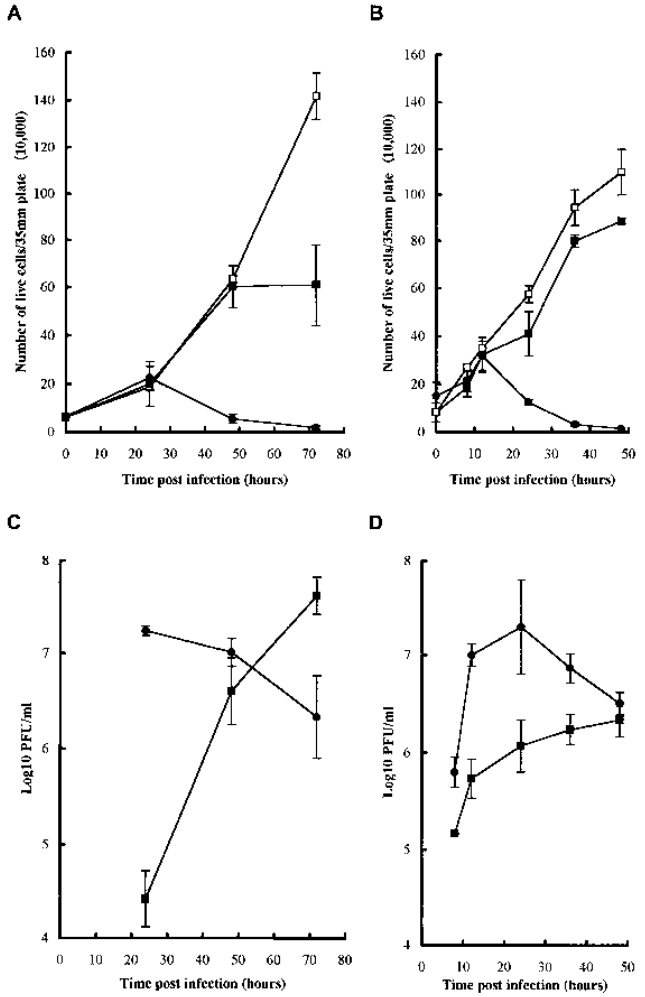

FIG. 3. Cell viability (A and B), determined by trypan blue exclusion of attached and floating cells, and accumulation of extracellular virus (C and D) in the clarified supernatant of AT3 cultures infected with SFV A7 (A and C) or SFV L10 (B and D). Each point represents the mean of three replicate cultures. The error bars indicate the standard deviations of the mean. The experiment was repeated at least three times with similar results. The drop in infectious virus titer in the supernatants of the SFV A7- and L10-infected AT3Neo cultures after 24 h postinfection represents virus instability at 37°C. □, uninfected AT3Bcl-2 cells; ■, infected AT3Bcl-2 cells; ●, infected AT3Neo cells.

However, by 30 h there was a marked difference in the number and distribution of virus antigen-positive cells in the cultures, with the majority of cells in infected AT3Neo cultures positive for viral glycoproteins but only relatively few cells positive in infected AT3Bcl-2 cultures (Fig. 5A and B, respectively). By 42 h, the number of viral antigen-positive cells in SFV A7-infected AT3Bcl-2 cultures had increased but still represented a small proportion of the culture. SFV L10 infection of AT3Bcl-2 cultures was similarly limited. Viral antigen-positive cells were not evenly scattered throughout infected AT3Bcl-2 cultures but tended to appear as isolated groups of viral antigen-positive cells within the largely viral antigen-negative monolayer. Occasionally, blebbing cells were observed within these limited areas of antigen-positive cells. Viral antigen-positive blebbing cells were more common in SFV L10-infected AT3Bcl-2 cultures. To eliminate the possibility that the AT3Bcl-2 cells which were positive for viral glycoproteins were cells which had lost *bcl-2* expression, cultures were double labeled for viral glycoproteins (Fig. 5H and I) and Bcl-2 protein (Fig. 5G and I). All cells in the culture, including those positive for viral glycoproteins, expressed Bcl-2 (Fig. 5G and I; Fig. 6A and B). The distribution of Bcl-2 was predominantly perinuclear (Fig. 6C).

In situ hybridization for viral RNA. To investigate the stage at which *bcl-2* interfered with SFV infection, the number of cells positive for viral RNA in SFV A7-infected AT3Bcl-2 and AT3Neo cultures relative to the number expressing viral antigen was determined by double labeling of the cultures, using in situ hybridization for viral RNA and immunostaining for viral glycoproteins. Cells which were positive for viral RNA and glycoproteins were rare in both cell lines up to 12 h. However, by 30 h, 98% of AT3Neo cells were positive for viral RNA, compared to only 3% of AT3Bcl-2 cells (Table 1). The percentage of viral RNA-positive cells in AT3Bcl-2 cultures increased to 17% by 42 h. As expected, in both cultures there were more viral RNA-positive cells than viral protein-positive cells. However, the proportions of viral RNA-positive to viral protein-positive cells were similar in the two cultures at all time points tested, indicating that there was no translational block in viral replication in the AT3Bcl-2 cultures.

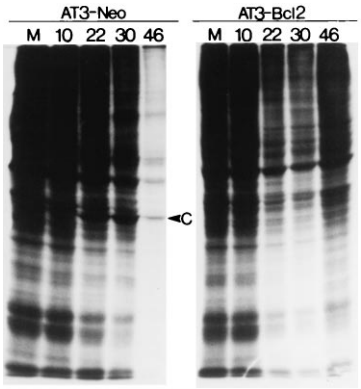

FIG. 4. Protein synthesis in SFV A7-infected AT3Neo and AT3Bcl-2 cells. Cell monolayers were either mock infected (lanes M) or infected with 5 PFU of SFV A7 per cell and then pulse-labeled for 1 h with ^{35}S-Trans-label (ICN) at 10, 22, 30, and 46 h postinfection. Cell lysates were fractionated on sodium dodecyl sulfate–12% polyacrylamide gels. The viral capsid protein (C) is indicated. In the AT3Neo cultures, this is first clearly apparent at 22 h. By 42 h, there is shutoff of host cell protein synthesis in these cultures. No capsid protein was detectable in the AT3Bcl-2 cultures, even at 46 h.

TUNEL and immunostain analysis. To further characterize the infection at the level of individual cells, cultures parallel to those double labeled for viral protein and viral RNA were double labeled for viral protein and TUNEL, and the number of blebbing cells was recorded (Table 1). By 30 h, the percentages of viral RNA-positive and viral glycoprotein-positive cells in SFV A7-infected AT3Neo cultures were 98 and 68%, respectively; 8% of the cells were TUNEL positive, and 5% were blebbing. In *bcl-2*-expressing cultures at this time point, only 3% of cells were viral RNA positive and only 2% expressed viral antigen. In both cultures, infected cells were rounded and shrunken relative to uninfected cells. The degree of rounding was proportional to the intensity of staining for viral glycoprotein. In SFV A7-infected AT3Bcl-2 cultures, TUNEL-positive and blebbing cells were only rarely observed (Table 1); however, the cytoplasm of viral antigen-positive AT3Bcl-2 cells often appeared to be particularly heavily laden with viral glycoproteins (Fig. 5B). It was striking that the proportion of cells with TUNEL-positive nuclei in the infected AT3Neo monolayers did not rise above 10% even when rapid cell death was ongoing in the culture, as seen, for example, at 42 h, when the viability of the culture was only 35%. It seems likely that fragmented nuclear DNA, in cells undergoing virus-induced apoptosis, can be end labeled only during a relatively brief phase in the apoptotic process. Likewise, the total number of cells displaying the classical apoptotic blebbing morphology at 42 h amounted to less than 5% of the culture. This result is in line with the execution phase of apoptosis being brief and the condemned phase being variable, resulting in an asynchronous transition through apoptosis (5).

Persistent infection. Monolayers from SFV A7- and SFV L10-infected AT3Bcl-2 cultures were transferred, after 72 h of infection, from the 35-mm-diameter dishes in which infections were initiated to T175 tissue culture flasks. Prior to transfer, the monolayers were washed with PBS, trypsinized briefly, and harvested into fresh medium. The monolayers were subcultured at weekly intervals. Levels of extracellular virus in the supernatants of SFV A7- and SFV L10-infected cultures reached 10^6 and 50 PFU/ml, respectively, at the end of the first passage and 10^5 and 4×10^4 PFU/ml, respectively, at the end of the second passage. The sparse remains of SFV L10-infected AT3Neo cultures were also transferred to T25 flasks with fresh medium. Colonies of cells were established from the few surviving cells and grew to form a monolayer. This culture of AT3Neo cells was subcultured in parallel to the persistently infected cell lines. No virus was detected in the supernatant from these cultures.

Cells from the first passage level of the AT3Bcl-2 culture persistently infected with SFV A7 were cytospun onto Biobond-coated glass slides, and in situ hybridization for viral RNA, immunostaining for viral glycoprotein, and TUNEL staining for DNA fragmentation were carried out (Table 1 and Fig. 5F). A small proportion (5%) of the AT3Bcl-2 cells were viral RNA positive, and many of these cells (3% of the total cell population) expressed viral glycoprotein. A small proportion (0.8%) of cells were TUNEL positive, and 0.2% of the cells displayed a blebbing morphology (Table 1). All cells in the culture, including those that were viral RNA and viral glycoprotein positive, expressed Bcl-2. It therefore appears that *bcl-2* can convert a normally lytic SFV infection to a persistent infection. The persistently infected culture exists as a chronically infected cell population in which the majority of cells are not undergoing productive viral replication. The infectious virus released into the culture supernatant originates from a subpopulation of productively infected cells. Individual productively infected cells within the persistently infected culture eventually die.

DISCUSSION

We have demonstrated that SFV infection induces morphological alterations in AT3Neo cells characteristic of apoptosis, including condensed and fragmented chromatin which is marginalized to the periphery of the nucleus and the replacement of the normal fine villus folds of a healthy cell membrane with dramatic bulges containing blebbing cytoplasm. The protruding blebs often contain high concentrations of viral glycoproteins. These observations are consistent with studies on Sindbis virus (18, 25).

Apoptosis in AT3Neo cultures proceeded more slowly with SFV A7 than with SFV L10. This result is consistent with the observation that SFV L10 displays greater cytopathogenicity for neuroblastoma cells than SFV A7 (2). AT3 cells overexpressing *bcl-2* displayed a markedly different response to SFV infection. Monolayers of AT3Bcl-2 cells survived infection with both the A7 and L10 strains of SFV, and persistently infected cell lines could be readily maintained after infection of AT3Bcl-2 cultures with both strains of virus. Overexpression of *bcl-2* has been shown to protect AT3 cell cultures from the lethal effects of infection with avirulent but not neurovirulent strains of Sindbis virus (18, 28). Studies with recombinant Sindbis viruses identified a single amino acid change (Gln in place of His at position 55 of the E2 glycoprotein) which conferred both neurovirulence and the ability to kill cells expressing *bcl-2* (28). Our studies suggest that the neurovirulence determinants which distinguish the A7 and L10 strains of SFV are unrelated to responsiveness to *bcl-2*. Similarly, neurovirulent strains of influenza virus cannot overcome the protective effect of *bcl-2* (11).

The survival of infected AT3Bcl-2 cultures resulted in levels of released virus accumulating to eventually exceed the maximum level of virus produced before death of the AT3Neo cultures. This finding illustrates the advantage that an apoptotic cell response can provide to a multicellular host by limiting virus yields. However, in vivo, by counteracting virus-encoded death signals, host-encoded antiapoptotic genes may be important to sustain the life of irreplaceable cells, perhaps long enough to enable non-cytopathic-immune mechanisms to clear

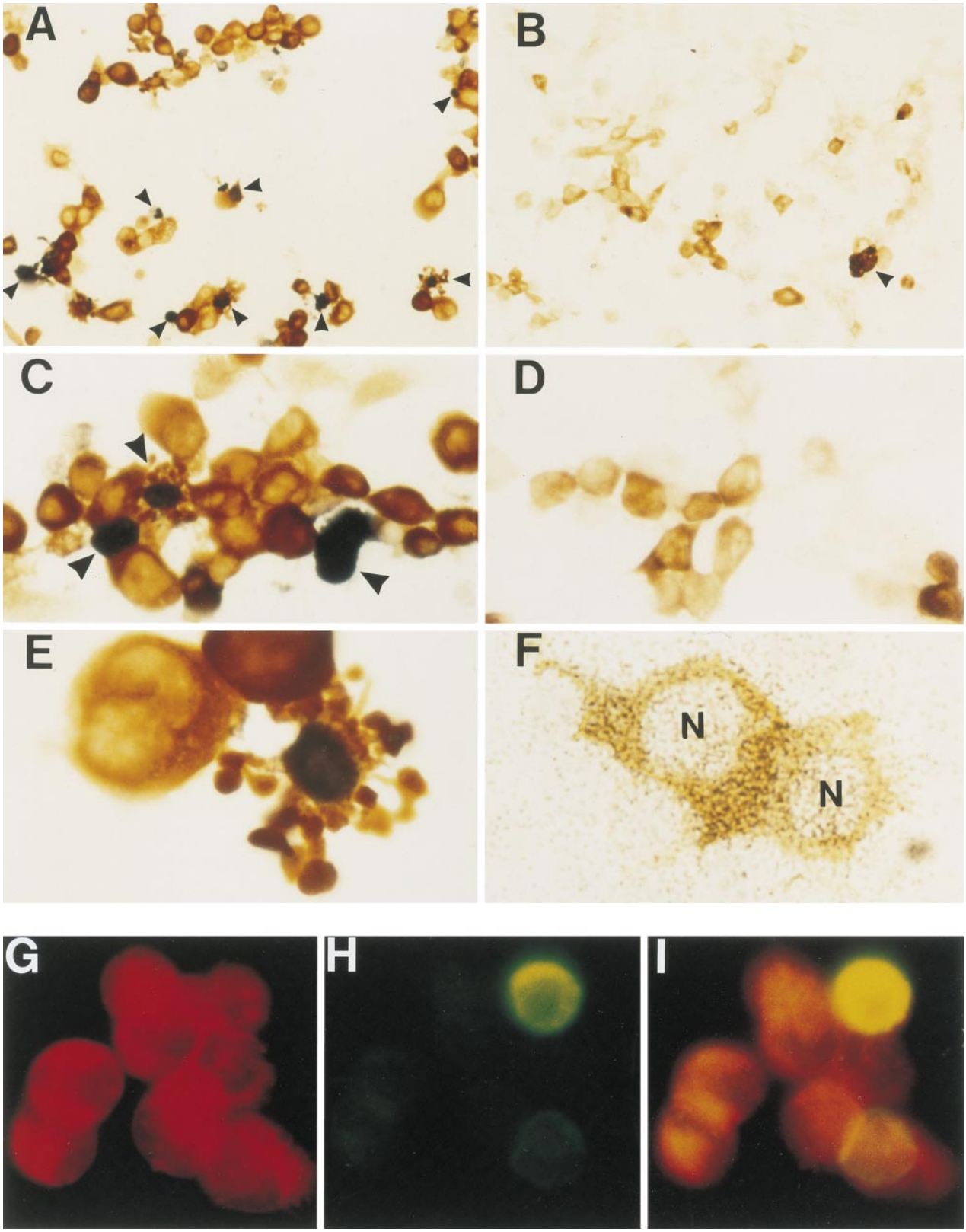

FIG. 5. Double-labeling studies of SFV-infected AT3Neo and AT3Bcl-2 cultures. (A to E) Immunostaining (brown) for the viral E1 and E2 envelope glycoproteins and TUNEL labeling (blue-black) for DNA fragmentation at 30 h after infection with SFV A7; (F) immunostaining (brown) for viral E1 and E2 proteins and in situ hybridization (silver grains) for viral RNA performed on cells from an AT3Bcl-2 culture persistently infected with SFV A7; (G to I) double immunostaining for Bcl-2 (red) and viral E1 and E2 proteins (green). (A, C, and E) AT3Neo cultures; (B and D) parallel AT3Bcl-2 cultures 30 h after SFV A7 infection. By 30 h, many cells in the AT3Neo cultures have been lost from the monolayer (A) and the majority of cells remaining on the monolayer are positive for viral glycoproteins (A and C). Most of the cells in the AT3Bcl-2 cultures remained on the monolayer, and only a small proportion of these (Table 1) stained positive for viral E1 and E2 proteins

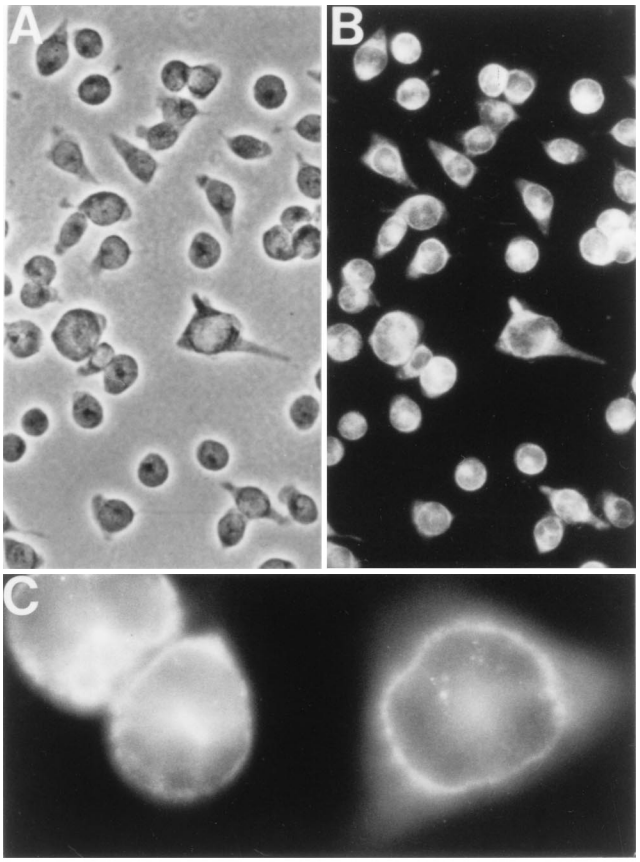

FIG. 6. Immunofluorescent labeling of AT3Bcl-2 cultures for Bcl-2 expression. As can be seen by comparison of the phase-contrast (A) and fluorescent (B) images of the same field, all cells in the AT3Bcl-2 culture stained strongly positive for Bcl-2. The staining was predominantly perinuclear (C).

TABLE 1. Percentages of cells in SFV A7-infected AT3Neo and AT3Bcl-2 cultures which were viral RNA positive, viral antigen positive, TUNEL positive, or displayed cytoplasmic blebs

Cell culture[a]	% Positive cells			
	Virus RNA	Virus antigen	TUNEL	Blebbing cells
30 h				
Neo (Un)	0	0	2	0
Neo A7(74)	98	68	8	5
Bcl-2 (Un)	0	0	0.2	0
Bcl-2 A7(74)	3	2	0.2	0.2
42 h				
Neo (Un)	0	0	0	0
Neo A7(74)	95	81	8	4
Bcl-2 (Un)	0	0	0	0
Bcl-2 A7(74)	17	14	0.3	0
PI				
Bcl-2 A7(74)	5	3	0.8	0.2

[a] Un, uninfected cells; PI, cells from the first passage level of the persistently infected cell line.

the infection. Noncytopathic, antibody-mediated clearance of alphavirus from CNS neurons has been demonstrated (17).

The explanation for the survival of the *bcl-2*-expressing cultures may be complex. If we exclude the unlikely but uninvestigated possibility that the two clones of AT3 cells differ phenotypically in factors other than *bcl-2* which affect virus replication and/or induction of cell death, then at least two aspects are clear. First, as demonstrated by the pulse-labeling, immunostaining, and in situ hybridization studies, overexpression of *bcl-2* affects virus entry or an early stage in virus replication, which results in very few cells in these cultures undergoing productive virus replication. There was a profound difference in the number of productively infected cells within monolayer cultures of AT3Neo relative to AT3Bcl-2 cells. However, there was no difference between these cultures in the proportion of viral glycoprotein-positive cells relative to viral mRNA-positive cells. This result indicates that the low number of productively infected AT3Bcl-2 cells does not result from a block in viral translation in the remaining majority of cells. Neither is *bcl-2* likely to be acting posttranslationally in these cells to limit virus assembly or release and therefore spread of infection in the culture. The extracellular virus released from the AT3Bcl-2 cultures represents an efficient yield from the relatively small number of virus glycoprotein-positive cells, and based on plaque size, this virus plaques with an efficiency equal to that of the purified input virus. The titers of infectious virus in the supernatants of both the SFV A7- and L10-infected AT3Bcl-2 cultures were sufficient at infection (MOI = 5) and at 24 h and 48 h to infect all of the cells in the culture, yet only a relatively small proportion showed evidence of virus replication as determined by positivity for viral RNA (Table 1): at 42 h, 17% for SFV A7 in the AT3Bcl-2 cultures, relative to 95% in the AT3Neo cultures. Our data therefore indicate that *bcl-2* functions early in the virus life cycle to inhibit virus entry or early stages of virus replication. This inhibition is prior to, or at the stage of, transcription of the subgenomic RNA or replication of the genomic RNA, since the probe used in our in situ hybridization reproducibly detects replicating levels of both of these species of viral RNA. However, the in situ hybridization is unlikely to be able to detect single copies of viral RNA, and we therefore cannot distinguish between the possibilities that the majority of the AT3Bcl-2 cells were infected but could not undergo the early stages of viral replication or that intact viral RNA did not enter the cytoplasm of these cells. Similarly, *bcl-2* expression has been reported to restrict influenza virus infection in transfected Madin-Darby canine kidney cell cultures (22). Bcl-2 therefore results in an early, entry-level, pretranscriptional or transcriptional block in SFV replication, which at least in some cells, or perhaps in all cells with time, can be overcome.

The second effect of *bcl-2* overexpression, which is clear and demonstrated by the culture survival curves (Fig. 3) and the TUNEL staining, is that cell death in the *bcl-2*-expressing cultures is delayed. This might be due to only a few cells being infected and triggered to die, although it is not clear how *bcl-2*

(B and D), some strongly (arrowhead). Several TUNEL-positive nuclei were observed in the infected AT3Neo cultures (arrowheads in panels A and C). The blebbing processes of these cells contained high levels of viral glycoproteins (E). TUNEL-positive cells were only rarely observed in the AT3Bcl-2 cultures (none are present in the fields shown). (F) AT3Bcl-2 cells double labeled for viral RNA (silver grains) and viral glycoproteins (brown immunostain) from the first passage level of a culture persistently infected with SFV A7. The nucleus (N) is unstained. (G to I) Double-immunofluorescent staining of SFV L10-infected AT3Bcl-2 cultures at 72 h, demonstrating that cells staining positive for viral E1 and E2 glycoproteins (green) have not lost their ability to express Bcl-2 (red). All cells in the culture were positive for Bcl-2. (I) Double exposure of fluorescence from Bcl-2 and viral antigen staining.

expression might affect virus entry. Alternatively, and perhaps more likely, many cells could be nonproductively infected. In this case, the viral trigger for induction of cell death must be downstream of the *bcl-2*-induced block in virus replication. Nevertheless, some cells in the AT3Bcl-2 cultures are productively infected. Whether *bcl-2* delays apoptosis in these cells is difficult to ascertain without knowing the time of infection and death of individual cells. In the SFV A7-infected AT3Bcl-2 cultures by 42 h, 17 and 14% of cells were virus RNA positive and virus protein positive, respectively (Table 1), but TUNEL-positive cells were rarely observed, and no difference in the growth curves of the infected and mock-infected cells was observed at this or earlier time points (Fig. 3). Furthermore, some of the cells in the AT3Bcl-2 cultures which were virus protein positive were more strongly positive than infected AT3Neo cells (Fig. 5B). These unusually high levels of viral proteins could result from prolonged cell survival. *bcl-2* expression therefore appears not only to inhibit an early stage of virus replication but also to buffer the death stimulus associated with SFV infection, slowing the rate of cell death rather than preventing it. In conclusion, *bcl-2* restricts SFV replication by inhibiting an early stage of the virus replication cycle and appears to prolong survival of productively infected cells. By altering the balance between productive virus replication-induced cell death and cell division, *bcl-2* expression promotes survival of the culture as a chronically infected cell population.

ACKNOWLEDGMENTS

We are grateful to Sylvia Shaw, Heather Dyson, and Yvonne Trozer for excellent technical support.

This work was supported by a grant from the UK Medical Research Council.

REFERENCES

1. **Amor, S., M. F. Scallan, M. M. Morris, H. Dyson, and J. K. Fazakerley.** 1996. Role of immune responses in protection and pathogenesis during Semliki Forest virus encephalitis. J. Gen. Virol. **77:**281–291.
2. **Atkins, G. J.** 1983. The avirulent A7 strain of Semliki Forest virus has reduced cytopathogenicity for neuroblastoma cells compared to the virulent L10 strain. J. Gen. Virol. **64:**1401–1404.
3. **Bradish, C. J., K. Allner, and H. B. Maber.** 1971. The virulence of original and derived strains of Semliki Forest virus for mice, guinea-pigs and rabbits. J. Gen. Virol. **12:**141–160.
4. **Cepko, C. L., B. E. Roberts, and R. C. Mulligan.** 1984. Construction and applications of a highly transmissible murine retrovirus shuttle vector. Cell **37:**1053–1062.
5. **Earnshaw, W. C.** 1995. Nuclear changes in apoptosis. Curr. Opin. Cell Biol. **7:**337–343.
6. **Esolen, L. M., S. W. Park, J. M. Hardwick, and D. E. Griffin.** 1995. Apoptosis as a cause of death in measles virus-infected cells. J. Virol. **69:**3955–3958.
7. **Fazakerley, J. K., S. Pathak, M. Scallan, S. Amor, and H. Dyson.** 1993. Replication of the A7(74) strain of Semliki Forest virus is restricted in neurones. Virology **195:**627–637.
8. **Fazakerley, J. K., P. Southern, F. Bloom, and M. Buchmeier.** 1991. High resolution in situ hybridization to determine the cellular distribution of lymphocytic choriomeningitis virus RNA in the tissues of persistently infected mice: relevance to arenavirus disease and mechanisms of viral persistence. J. Gen. Virol. **72:**1611–1625.
9. **Fazakerley, J. K., and H. E. Webb.** 1987. Semliki Forest virus-induced, immune-mediated demyelination: adoptive transfer studies and viral persistence in nude mice. J. Gen. Virol. **68:**377–385.
10. **Griffin, D. E., B. Levine, W. R. Tyor, P. C. Tucker, and J. M. Hardwick.** 1994. Age-dependent susceptibility to fatal encephalitis: alphavirus infection of neurons. Arch. Virol. **9:**31–39.
11. **Hinshaw, V. S., C. W. Olsen, N. Dybdahl-Sissoko, and D. Evans.** 1994. Apoptosis: a mechanism of cell killing by influenza A and B viruses. J. Virol. **68:**3667–3673.
12. **Johnson, R. T., H. F. McFarland, and S. E. Levy.** 1972. Age-dependent resistance to viral encephalitis: studies of infections due to Sindbis virus in mice. J. Infect. Dis. **125:**257–262.
13. **Kawanishi, M.** 1993. Epstein-Barr virus induces fragmentation of chromosomal DNA during lytic infection. J. Virol. **67:**7654–7658.
14. **Krajewski, S., J. K. Mai, M. Krajewski, M. Sikorska, M. Mossakowski, and J. C. Reed.** 1995. Upregulation of Bax protein levels in neurons following cerebral ischemia. J. Neurosci. **15:**6364–6376.
15. **Laemmli, U. K.** 1970. Cleavage of structural proteins during the assembly of the head of bacteriophage T4. Nature **227:**680–685.
16. **Laurent-Crawford, A. G., B. Krust, S. Muller, Y. Riviere, M.-A. Rey-Cullie, J.-M. Bechet, L. Montagnier, and A. G. Hovanessian.** 1991. The cytopathic effect of HIV is associated with apoptosis. Virology **185:**829–839.
17. **Levine, B., J. M. Hardwick, B. D. Trapp, T. O. Crawford, R. C. Bollinger, and D. E. Griffin.** 1991. Antibody-mediated clearance of alphavirus infection from neurons. Science **254:**856–860.
18. **Levine, B., Q. Huang, J. T. Isaacs, J. C. Reed, D. E. Griffin, and J. M. Hardwick.** 1993. Conversion of lytic to persistent alphavirus infection by the *bcl-2* cellular oncogene. Nature **361:**739–742.
19. **Meyaard, L., S. A. Otto, R. R. Jonker, M. J. Miinster, R. P. M. Keet, and F. Miedema.** 1992. Programmed death of T cells in HIV-1 infection. Science **257:**217–219.
20. **Morey, A. L., D. J. P. Ferguson, and K. A. Flemming.** 1993. Ultrastructural features of fetal erythroid precursors infected with parvovirus B19 in vitro: evidence of cell death by apoptosis. J. Pathol. **169:**213–220.
21. **Oliver, K. R., M. F. Scallan, H. Dyson, and J. K. Fazakerley.** Susceptibility to a neurotropic virus and its changing distribution in the developing brain is a function of CNS maturity. J. Neurovirol., in press.
22. **Olsen, C. W., J. C. Kehren, N. R. Dybdahl-Sissoko, and V. S. Hinshaw.** 1996. *bcl-2* alters influenza virus yield, spread, and hemagglutinin glycosylation. J. Virol. **70:**663–666.
23. **Pathak, S., and H. E. Webb.** 1978. An electron-microscopic study of avirulent and virulent Semliki forest virus in the brains of different ages of mice. J. Neurol. Sci. **39:**199–211.
24. **Pathak, S., H. E. Webb, S. W. Oaten, and S. Bateman.** 1976. An electron-microscopic study of the development of virulent and avirulent strains of Semliki Forest virus in mouse brain. J. Neurol. Sci. **28:**289–300.
25. **Rosen, A., L. Casciola-Rosen, and J. Ahearn.** 1995. Novel packages of viral and self-antigens are generated during apoptosis. J. Exp. Med. **181:**1557–1561.
26. **Smyth, J. M. B., B. J. Sheahan, and G. J. Atkins.** 1990. Multiplication of virulent and demyelinating Semliki Forest virus in the mouse central nervous system: consequences in BALB/c and SJL mice. J. Gen. Virol. **71:**2575–2583.
27. **Tolskaya, E. A., L. I. Romanova, M. S. Kolesnikova, T. A. Ivasnikova, E. A. Smirnova, N. T. Raikhlin, and V. I. Agol.** 1995. Apoptosis-inducing and apoptosis-preventing functions of poliovirus. J. Virol. **69:**1181–1189.
28. **Ubol, S., P. C. Tucker, D. E. Griffin, and J. M. Hardwick.** 1994. Neurovirulent strains of alphavirus induce apoptosis in bcl-2 expressing cells; role of a single amino acid change in the E2 glycoprotein. Proc. Natl. Acad. Sci. USA **91:**5202–5206.